Published in final edited form as:
Cancer Res. 2008 December 1; 68(23): 9918–9927. doi:10.1158/0008-5472.CAN-08-1718.

Crosstalk between the Androgen Receptor and β-Catenin in Castrate Resistant Prostate Cancer

Gang Wang[1], **Jun Wang**[1], and **Marianne D. Sadar**[1,*]

1*Genome Sciences Centre, British Columbia Cancer Agency, 600 West 10th Avenue, Vancouver, British Columbia, V5Z 4E6, Canada*

Abstract

The androgen-signaling pathway plays an important role in the development and hormonal progression of prostate cancer to the castrate resistant stage (also called androgen-independent or hormone refractory). The Wnt pathway and β-catenin contribute to prostate biology and pathology. Here application of Affymetrix Genechip analysis revealed the genomic similarity of the LNCaP hollow fiber model to clinical samples and identified genes with differential expression during hormonal progression. The fiber model samples clustered according to the expression profile of androgen-regulated genes to provide genomic evidence for the reactivation of the AR signaling pathway in castrate resistant prostate cancer. Pathway based characterization of gene expression identified activation of the Wnt pathway. Together with the increased expression of AR and β-catenin, there was increased nuclear colocalization and interaction of endogenous AR and β-catenin in castrate resistant prostate cancer from castrated mice. Surprizingly no interaction or colocalization of AR and β-catenin could be detected in xenografts from non-castrated mice. These studies provide the first *in vivo* evidence to support aberrant activation of the AR through the Wnt/β-catenin signaling pathway during progression of prostate cancer to the terminal castrate resistant stage.

Keywords

androgen receptor; beta-catenin; crosstalk; hormonal progression; prostate cancer

Introduction

Androgen ablation is currently the most effective systematic therapy available for prostate cancer patients with metastatic disease. However this therapy is palliative and after an initial response to androgen ablation, most tumors eventually begin to grow in the absence of testicular androgens to form castrate resistant disease (1). Molecular mechanisms underlying hormonal progression to the castrate resistant stage remain unknown. One mechanism suspected to play a role is related to the transcriptional activity of the androgen receptor (AR). The AR is a ligand-dependent transcription factor that is a member of the steroid receptor family. Ligand-activated AR, complexed with coactivator proteins and general transcription factors, bind to androgen response elements (AREs) located in the promoter and enhancer regions to activate or repress the transcription of specific target genes suspected to be involved in proliferation.

One important coregulator of the AR is β-catenin which interacts with the AR in response to androgen to increase the transcriptional activity of the AR in cells maintained as a monolayer

*Correspondence should be addressed to: Marianne D Sadar, Genome Sciences Centre, BC Cancer Research Centre, 675 West 10th Avenue, Vancouver, BC, CANADA, V5Z 1L3, Tel: 604-675-8157, FAX: 604-675-8178, email: msadar@bcgsc.ca.

(2,3). Levels of β-catenin and AR are both increased in castrate resistant prostate cancer. Mutated forms of β-catenin which can result in a stabilized protein have also been detected in prostate cancer (4,5). β-catenin has dual functions that involve both cell adhesion and signal transduction in response to Wnt ligands (6,7). The cellular localization of β-catenin is important for its function. Consistent with its role in cell adhesion, β-catenin is predominantly detected at the cell membrane where it interacts with E-cadherin and α-catenin (8). In response to Wnt ligands, β-catenin can also be detected in the nucleus and cytoplasm where it can interact with TCF/LEF transcription factors to initiate transcription of target genes such as c–myc and cyclin D1 (9–11). β-catenin activity is regulated by phosphorylation followed by degradation. This process involves interaction with GSK3β, axin, and adenomatous polyposis coli (APC). Phosphorylation of β-catenin by CK1ε and GSK3β on serine and threonine residues target it for degradation by the ubiquitin proteasome pathway (12). Degradation of β-catenin is inhibited by Wnt signaling which results in elevation of levels of β-catenin in the nucleus and interaction with Tcf/Lef transcription factors to regulate expression of target genes (9,13).

Crosstalk between Wnt and AR pathways occurs at several levels: 1) Wnt ligands can transactivate the AR (14); 2) β-catenin interacts with the AR to increase its transcriptional activity as measured by androgen-induced reporter gene constructs (2,3,15–17); 3) GSK3β negatively regulates AR-mediated transcription (18–20); 4) competition for β-catenin can occur between AR and Tcf/Lef (21); and 5) the Tcf/Lef target gene, cyclin D1, can interact with the AR to inhibit AR transcriptional activity (22–24).

In the present study, we applied Affymetrix GeneChip (Human Genome U133 plus 2) combined with the LNCaP xenograft and Hollow Fiber models to identify global changes in gene expression changes associated with castrate resistant prostate cancer. One pathway identified to be activated in castrate resistant samples was the Wnt/β-catenin signaling pathway. Colocalization and interaction of AR and β-catenin were detected for the first time *in vivo* in castrate resistant tumors, but surprisingly not from tumors harvested from non-castrated mice. These data suggest a role for β-catenin interaction with the AR in the progression of prostate cancer to the terminal castrate resistant stage.

Materials and Methods

Hollow Fiber and subcutaneous xenograft models of prostate cancer

The LNCaP Hollow Fiber model of prostate cancer was performed as described previously (25,26). Subcutaneous xenografts were prepared in male SCID mice inoculated with about 1×10^6 LNCaP cells suspended in 75 μl of RPMI 1640 (5% FBS) with 75 μl of Matrigel (Becton Dickinson Labware) in the flank region using a 27 gauge needle. Tumor volumes of xenografts were measured weekly and calculated by the formula LxWxHx0.5236. Serum PSA levels were measured weekly as reported previously (25,26).

RNA isolation and microarray analysis

RNA was isolated and analyzed using microarrays as described previously (26). Briefly, total RNA was extracted from cells using Trizol (Invitrogen Life Technologies, Carlsbad, CA) according to the manufacturer's protocol. RNA samples from cells were analyzed by Affymetrix Genechip microarray. The syntheses of cDNA and biotinylated cRNA were performed according to the protocols provided by the manufacturer (Affymetrix, Santa Clara, CA). Biotinylated fragmented cRNA probes were hybridized to the HGU133 plus2 Genechips (Affymetrix). Hybridization was performed at 45°C for 16h in a hybridization oven (Affymetrix). The Genechips were automatically washed and stained with streptavidin–phycoerythrin conjugate in an Affymetrix Genechip Fluidics Station. Fluorescence intensities

were scanned with a GeneArray Scanner (Affymetrix). Hybridizations were carried out independently for each condition using 3 biological replicates.

Expression profile analysis

Comparative analyses between expression profiles for Affymetrix experiments were carried out using GeneSpringTM software version 7.2 (Silicon Genetics, CA, USA). The expression profiles from three animals were compared using two-way ANOVA to identify genes that were differentially expressed across the three groups. The dataset, GEO GDS1390, for clinical samples of androgen-dependent and castrate resistant prostate cancer was downloaded from PUBMED. For sample clustering, standard correlation was applied to measure the similarity of the expression pattern between different samples. Class prediction was performed to calculate the similarity of the samples from the LNCaP hollow fiber model to the clinical samples of castrate resistant prostate cancer.

Quantitative RT–PCR (qRT–PCR)

Oligo-d(T)-primed total RNAs (0.5 μg per sample) were reverse-transcribed with SuperScript III (Invitrogen Life Technologies, Carlsbad, CA, USA). An appropriate dilution of cDNA and gene-specific primers were combined with SYBR Green Supermix (Invitrogen) and amplified in ABI 7900 real-time PCR machine (Applied Biosystems, Foster City, CA, USA). All qPCR reactions were performed in triplicate. The threshold cycle number (Ct) and expression values with standard deviations were calculated in Excel. Primer sequences for real-time PCRs are listed in **SI Table 1**. Real-time amplification was performed with initial denaturation at 95°C for 2 min, followed by 40 cycles of two-step amplification (95°C for 15 sec, 55°C for 30 sec).

Whole-cell lysates and western blot analyses

Protein from whole-cell lysate was isolated using Trizol according to the manufacturer's protocol. Samples were stored at −80°C until use. The antibodies used in these studies were obtained from various suppliers: AR (PG21, Upstate Biotechnology, Lake Placid, NY, USA); PSA (C-19, Santa Cruz, Santa Cruz, CA, USA); β-catenin (Cell Signaling, Danvers, MA, USA); phospho-Y142 β-catenin (Abcam, Cambridge, MA, USA); β-actin (Abcam); Gsk3β (Abcam); CTNNBIP1 (Abcam); Cyclin D1 (Abcam); p53 (Abcam); and Tcf3 (Abcam).

Immunoprecipitation

Protein was extracted from LNCaP cells or xenograft tumor samples using Triton X-100 lysis buffer (150 mM NaCl, 1% Triton X-100, 50 mM Tris HCl). The cell lysates of the xenografts were stripped of albumin by using Montage Albumin Deplete Kit (Millipore, Billerica, MA, USA). A total of 250 μg of cell lysate per immunoprecipitation were used to immunoprecipitate AR using anti-AR antibody (PG21, Upstate Biotechnology, Lake Placid, NY, USA) or β-catenin using an anti-β-catenin antibody (Cell Signaling, Danvers, MA, USA) with μMACS protein G Microbeads (Miltenyi Biotec, Auburn, CA, USA). Proteins were detected by western blot analysis using anti-AR and anti-β-catenin antibodies.

Double immunofluorescent microscopy

Tissue sections (5 μm) were blocked in immunohistochemistry solution (Immunovision Technologies, Brisbane, CA) and immunostained with anti-AR antibody (AR441, Santa Cruz, CA, USA) (1:10) at 4° C overnight, then anti-β-catenin antibody (Cell Signaling, Danvers, MA, USA) (1:20) at 4° C overnight. For immunofluorescence staining, sections were incubated with fluorescein isothiocyanate (FITC)-labelled anti-rabbit IgG for β-catenin and tetramethylrhodamine isothiocyanate (TRITC)-labeled anti-mouse IgG for AR (both 1:200) for 30 min. The immunofluorescence staining of proteins was detected using a Zeiss Axioplan-2 Fluorescence Microscope (Zeiss, Toronto, ON, Canada).

Results

The LNCaP hollow fiber model correlates to clinical hormonal progression of prostate cancer

The LNCaP hollow fiber model provides a reproducible method to obtain human prostate cancer cells that are free from host contamination from *in vivo* studies (25). A strength of this model is that it allows analyses of matched samples from the same animal at different time points due to the noninvasive procedures to harvest the fibers. Here we apply this model to obtain protein and RNA from LNCaP cells harvested from castrated mice during the different stages of progression to assess changes in gene expression and identify pathways associated with castrate resistant growth. Consistent with previous reports, LNCaP cells maintained in hollow fibers progressed to castrate resistant after castration of the host as indicated by levels of serum PSA (Fig 1A). The removal of fibers from the animals is indicated by the arrows and caused further reduction in serum PSA due to the removal of tumor cells. Serum PSA levels are correlated to tumor burden (27). At least a three-fold increase in serum PSA over the nadir level was still observed in spite of removal of fibers to indicate castrate resistant re-expression of PSA at 31 days after castration. Analyses of levels of PSA mRNA and PSA protein (Fig 1A) from LNCaP cells harvested from fibers immediately prior to castration (intact or androgen dependent, AD), after castration at the PSA nadir (androgen ablation or AA), or 31 days after castration when serum PSA becomes elevated again (castrate resistant or AI) were consistent with hormonal progression in response to castration. PSA mRNA and protein were reduced by approximately 80% in response to castration (AA) as compared to levels from samples harvested from intact mice (AD). Levels of expression of PSA mRNA and protein returned to pre-castrate levels in castrate resistant samples (compare levels in AD to AI in Fig 1A). These samples were next used for Affymetrix analysis of changes in the transcriptome during hormonal progression and expression profiles compared to Affymetrix data available for clinical samples of prostate cancer.

To confirm the similarity of the castrate resistant samples harvested from the hollow fiber model to clinical samples, we screened a group of the most significantly differentially expressed genes in the clinical samples composed of both androgen-dependent and castrate resistant prostate cancers (28). There were 79 genes identified to be significantly differentially expressed between castrate resistant versus androgen-dependent clinical samples with the p-value lower than 0.001 (**SI Table 2**). A hierarchical two-dimensional clustering algorithm based on similarity of expression patterns was applied to these 79 genes. Comparison of expression profiles demonstrated a tendency to subgroup the castrate resistant samples from the fiber model together with the clinical castrate resistant prostate cancers, while the androgen-dependent from the fiber model clustered together with the clinical androgen-dependent prostate cancers (Fig. 1B). The class prediction analysis revealed the androgen ablation and castrate resistant samples from the fiber model have positive similarity scores to the clinical castrate resistant prostate cancers, but castrate resistant samples have significant more similarity scores than the androgen ablation samples ($p<0.05$) (Fig. 1C). These data provide evidence that the LNCaP hollow fiber model is a relevant model to study hormonal progression of prostate cancer.

Global gene expression profiles of hormonal progression of prostate cancer

After confirmation of similarity between the hollow fiber model and the clinical samples at the transcriptome level, significance analysis of microarrays (29) was applied to identify genes differentially expressed across the different stages of hormonal progression. Using a two-way analysis of variance ($P<0.05$), 5667 genes were measured as differentially expressed across the various time points (Fig. 2). These 5667 genes were further clustered by standard correlation according to the expression pattern during the hormonal progression to castrate resistant disease. Cluster 1 (represented by CTNNBIP, a regulator of β-catenin) included 814 genes

whose expression increased in castrate resistant samples. Cluster 2 (represented by OSR2, β-catenin (CTNNB1), and AR) included 1143 genes whose expression increased after castration, and further increased or remained elevated in castrate resistance. Cluster 3 (represented by MMP16 and Wnt5A) included 489 genes whose expression increased after castration, but decreased in castrate resistance. Cluster 4 (represented by androgen regulated genes Dlc2 and FKBP5, TP53, GSK3B, LEF1 and TCF3) included 1540 genes whose expression decreased in response to castration and remained decreased in castrate resistance. Cluster 5 (represented by CSNK2B, CSNK1E, CCND1, MYC, and PLCB4) included 1226 genes whose expression decreased only when the tumor progressed to castrate resistance. Cluster 6 (represented by androgen regulated genes KLK3, KLK2, ELL2, SOCS2 and RHOU) included 455 genes whose expression decreased in response to castration, but increased in castrate resistant samples.

Reactivation of the AR pathway in castrate resistant prostate cancer

Hormonal progression of prostate cancer has been suggested to be at least partially due to the reactivation of AR after androgen ablation therapy (30). To characterize the status of the AR pathway in castrate resistant prostate cancer, a hierarchical two-dimensional clustering algorithm that was based on similarity of expression patterns was applied to 1092 genes previously identified to be differentially expressed in response to androgen in LNCaP cells maintained in cell culture (26). The genes are represented on each row (Fig 3) and experimental samples are represented on each column. Comparison of expression profiles demonstrated a strong tendency to subgroup the samples with respect to the stage of the tumors. This suggested that distinct and consistent differences in the levels of transcript occurred during hormonal progression. Of particular interest, hierarchical cluster analysis revealed that the expression patterns of androgen-regulated genes in castrate resistant samples were more similar to that of the androgen-dependent than to androgen ablation samples. These data are consistent with re-expression of some androgen-regulated genes in castrate resistant prostate cancer xenografts obtained from castrated hosts as previously observed (31).

Increased expression of AR and β-catenin in castrate resistant prostate cancer

Genes differentially expressed in castrate resistant prostate cancer represented many biological categories; however, several of these genes have functional attributes that could contribute to castration-resistant growth. The most notable were the marked increase in levels of mRNA for AR ($p=0.04$) and β-catenin ($p=2.45E-05$) (Fig 4A) in the castrate resistant samples measured by both Affymetrix and Q-PCR. Western blot analysis confirmed increased levels of AR and β-catenin (Fig 4B) proteins in castrate resistant prostate cancer samples. These data are consistent with clinical data describing elevated expression of AR and β-catenin in hormone refractory prostate cancer.

Cytoplasmic or nuclear localization of β-catenin is required to mediate Wnt signaling. For β-catenin to accumulate in the cytoplasm, it requires phosphorylation on its tyrosine residue (Y142) to decrease interaction with α-catenin (12,32,33). Therefore levels of phosphorylated β-catenin were measured during the different stages of hormonal progression by western blot analyses with an antibody against phospho-Y142 of β-catenin. No phosphorylation of Y142 could be detected in samples from intact mice (Fig 4B). Androgen ablation increased phosphorylation of Y142-β-catenin to detectable levels which were further increased with castrate resistance. These data imply that the cellular localization of β-catenin may be altered with hormonal progression of prostate cancer to the cytoplasmic or nuclear form to mediate signal transduction.

Expression profile of members of the Wnt pathway in castrate resistant prostate cancer

β-catenin is the mediator of Wnt signal transduction pathway and its activity is regulated by many Wnt pathway members. To investigate the status of the Wnt pathway in the hormonal

progression of prostate cancer, we validated changes in the expression of some members of Wnt pathway during the prostate cancer progression as first indicated by Affymetrix data. Consistent with increased levels of Y142 phospho-β-catenin in castrate resistant prostate cancer, expression of tyrosine kinase-associated YES1 and LYN that phosphorylate β-catenin (33) were increased with castrate resistance (Fig. 4C). The β-catenin activator WNT2B was also significantly increased with castrate resistance. Consistent with activation of the β-catenin pathway in castrate resistant samples, the expression of β-catenin inhibitors such as CSNK2B, CSNK1E, GSK3B, TP53, WNT5A and PLCB4 were decreased (Fig. 4C). The β-catenin downstream transcription factors, TCF3 and LEF, and expression of their target genes, MYC and CCND1, were significantly decreased, while expression of the transcription inhibitor, CTNNBIP1, was increased in castrate resistant prostate cancer. Consistent with the mRNA level, the protein level of Ctnnbip1 is increased while the levels of p53, Tcf-3, Cyclin-D1 and Gsk3β are decreased in the castration resistant samples (Fig. 4D). Together these data are consistent with the hypothesis of an increased cytoplasmic pool of β-catenin without increased activity of its downstream transcription factors (TCF and LEF).

Increased colocalization of AR and β-catenin in castrate resistant prostate cancer

Activation of the Wnt pathway should induce the accumulation of β-catenin in cytoplasm which would be expected to facilitate the activity of downstream transcription factors. While we expect to see increased cytoplasmic or nuclear accumulation of β-catenin based upon elevated levels of phospho-Y142-β-catenin, we in fact measured a decrease in its downstream transcription factors and target genes in castrate resistant prostate cancer. One possible mechanism for why no concomitant increases in TCF/LEF target genes were measured may involve competition for β-catenin with the AR (21). To further explore for possible crosstalk between β-catenin and AR in castrate resistant prostate cancer, we investigated the colocalization of AR and β-catenin by fluorescent microscopy using xenografts harvested before and after castration. Tissue sections were prepared from xenografts harvested the day of castration, at the PSA nadir, and when samples were castrate resistant and stained using antibodies against AR and β-catenin. The staining pattern for AR in xenografts harvested from non-castrated mice was strongly nuclear as expected, while β-catenin staining was predominately at cell borders (Fig. 5A). After castration, the AR was diffuse in the cytoplasm with little detected within the nucleus, while β-catenin was still mainly at the cell borders with little cytoplasm diffusion and low colocalization with AR. Castrate resistant xenografts from castrated mice, showed nuclear localization of β-catenin in cells that predominately co-localized with AR (arrowheads). Levels of β-catenin at cell borders were not observed to change in different stages of prostate cancer, whereas cytoplasmic levels increased with progression. These data suggest that colocalization of AR and β-catenin only occurs *in vivo* in castrate resistant prostate cancer and contradictory to *in vitro* data, not in the presence of androgen in non-castrated mice.

Increased interaction between AR and β-catenin in castrate resistant prostate cancer

In cell culture, β-catenin interacts with the AR and acts as a coactivator to increase the transcriptional activity of the AR in response to androgen (2,3,15–17). To date all studies have examined these interactions using cells maintained as a monolayer with no *in vivo* reports. Since β-catenin interacts with molecules involved in cell adherence, it would seem that cells maintained in a monolayer may not provide the optimal model to predict what may occur in a tumor or spheroid structure. Thus here we provide the first *in vivo* study of interaction between AR and β-catenin. In addition this is also the first study to attempt to show changes in this interaction during hormonal progression; something that cannot be accurately mimicked *in vitro*. To do this, endogenous complexes of AR and β-catenin were co-immunoprecipitated from LNCaP xenografts at various stages of hormonal progression. Xenografts were harvested at the day of castration (intact mice), at the PSA nadir (castrated), and when castrate resistant,

and proteins immunoprecipitated using antibodies directed to β-catenin or AR. The immunoprecipitated complexes were probed by western blot analyses. Consistent with the lack of colocalization in the presence of androgen in non-castrated mice (Fig 5A), no interaction between AR and β-catenin was detected in the presence of androgen (Fig 5B). Importantly these data showed increased levels of endogenous AR/β-catenin complex from *in vivo* samples harvested from castrate resistant prostate cancer, compared to androgen-dependent and androgen ablation tissues (Fig. 5B). These data are in agreement with the colocalization studies shown in Fig 5A and together they suggest that AR interacts with β-catenin in castrate resistant prostate cancer.

Discussion

The Wnt/β-catenin pathway contributes to prostate biology and pathology. The AR is suspected to play an important role in castrate resistant prostate cancer. These two pathways may cross-talk in castrate resistant prostate cancer. The present studies investigated genes differentially expressed during the hormonal progression of prostate cancer and revealed the following: 1) the LNCaP hollow fiber model correlated with clinical hormonal progression of prostate cancer; 2) hormonal progression of prostate cancer in the hollow fiber model was associated with differential expression of 5,667 genes; 3) the expression pattern of androgen-regulated genes in castrate resistant prostate cancer was more similar to that obtained before castration compared to the tumors receiving androgen ablation at PSA nadir; 4) expression of AR and β-catenin were increased in castrate resistant prostate cancer; 5) nuclear colocalization and protein-protein interaction between the endogenous AR and endogenous β-catenin were increased in vivo in castrate resistant prostate cancer; and 6) deregulation of the Wnt pathway in castrate resistant prostate cancer led to dissociation of β-catenin from the cell membrane but not to activation of its downstream Tcf/Lef transcription factors.

The LNCaP hollow fiber model correlates to clinical hormonal progression of prostate cancer

A number of animal models are available to investigate the mechanisms underlying the development and pathogenesis of the prostate cancer. We developed an *in vivo* model that encompasses the use of hollow fibers to obtain tumor cells that were free from contamination with host cells and to allow harvesting of multiple samples from an individual mouse at different stages of progression (25). LNCaP cells seeded in fibers that were subcutaneously implanted into the mice provided measurable levels of serum PSA that decreased by 90% to a nadir after castration, and subsequently serum PSA increased within 4–5 weeks after castration signifying progression to androgen-independence (Fig. 1A). Data from this fiber model for both serum PSA and levels of PSA mRNA and protein were consistent with those data obtained with the LNCaP xenograft model (34). Condition clustering and the class prediction analysis provided support that the hollow fiber model mimics clinical samples at the level of global transcription during hormonal progression (Fig. 1B). These data provide the first evidence of similarity between the LNCaP hollow fiber model to the clinical scenario at the transcriptome level for hormonal progression.

Reactivation of AR pathway in castrate resistant prostate cancer

PSA is an example of an androgen-regulated gene that contains several well-characterized androgen response elements (AREs) in the promoter and enhancer regions to which the AR binds to initiate transcription (35–37). The re-expression of PSA suggests that the AR plays a role in castrate resistant disease. Affymetrix Genechip analysis identified changes in expression of 1,092 genes in response to androgen stimulation in LNCaP cells (26). Here we clustered the fiber model samples according to the expression profile of these androgen-regulated genes to investigate the status of AR pathway during the hormonal progression of prostate cancer. Surprisingly, in spite of the similar androgen environment as the androgen ablation samples,

the castrate resistant prostate cancer samples shared a more common expression profile of androgen-regulated genes with the androgen-dependent samples before castration (Fig. 3). Specific examples include the expression of androgen-regulated genes such as KLK3, KLK2, ELL2, SOCS2, and RHOU that were re-expressed in castrate resistant prostate cancer. Expression of genes that are known to be suppressed by androgen, such as MMP16 (26), were re-suppressed in castrate resistant prostate cancer (Fig 2). Together these data suggest reactivation of the AR in castrate resistant disease as previously suggested (38–40). Consistent with the reactivation of AR is the overexpression of AR. Levels of AR mRNA increased in AA samples (Figure 4A), while levels of AR protein remained similar compared to the AD samples (Figure 4B). This was expected due to increased stability of the AR protein in presence of androgen. One potential mechanism for re-activation of the AR in the absence of testicular androgen may involve changes in protein-protein interactions with coregulators in response to alternative signal transduction pathways. Some possible responsive signaling pathways and the AR interaction proteins have been reviewed recently (30) and include MAPK, Akt, PKC and PKA. These pathways may directly modify the AR or indirectly activate AR by modification of coactivators. β-catenin is such a coactivator of AR which may involved in the ligand independent activation of AR. In present study, we provide the first *in vivo* evidence of the relevance of β-catenin pathway in the hormonal progression of CaP.

β-catenin has been reported to be a relatively specific coactivator of the AR with only the vitamin D receptor of the steroid receptor family also showing some interaction (3). These studies are based upon over-expression of β-catenin to increase the transcriptional activity of the AR measured by reporter gene constructs in response to androgen (2,3). Chromatin immunoprecipitation assays detected β-catenin recruitment to the PSA promoter (41). In yeast cells exposed to dihydrotestosterone, repeat 6 of the armadillo repeats of β-catenin interacts with the AR ligand-binding domain (3). Interaction between β-catenin and the AR is reported to be dependent on androgen due to enhanced interaction upon the addition of ligand (2,3). These previous reports are based upon studies using cells maintained in culture as a monolayer which may not reflect *in vivo* conditions especially when considering the importance of adhesion molecules in modulating the function of β-catenin. Curiously we did not detect interaction of β-catenin with the AR *in vivo* in xenografts harvested from non-castrated mice. Instead we detected interaction between β-catenin and AR with hormonal progression in castrated mice (Fig. 5B), which was consistent with colocalization studies (Fig. 5A). These data are the first to show *in vivo* interactions between the AR and β-catenin and highlight potential discrepancies when extrapolating from solely *in vitro* experiments. The importance of validating endogenous complexes using *in vivo* physiological or pathological conditions is based upon: 1) protein-protein interactions are dependent upon concentrations of the proteins as well as the levels of stimulation, and thus overexpression of a protein by transfection may lead to false-positives; 2) over-expression or forced expression of proteins may cause aberrant cellular localization and/or inappropriate timing of expression if the expression of proteins are “normally” dependent upon the cell cycle phase; 3) protein modifications required for interactions may vary in different cells or under different cellular conditions; 4) cell cultures cannot substitute the physiological milieu of in vivo conditions nor can cell cultures mimic accurately the hormonal progression that occurs in vivo in response to castration of the host; and 5) the three-dimensional architecture of the xenograft and potential effects on E-cadherin and other cell adhesion molecules may not be accurately represented using cells maintained in monolayer. These points are especially important when investigating protein-protein interactions of the AR activated by non-androgenic pathways involving signal transduction pathways that may be not be accurately mimicked *in vitro*.

E-cadherin mediates cell-cell contact and regulates the levels of β-catenin localized in the cytoplasm with overexpression of E-cadherin causing redistribution of β-catenin to the cell membrane to reduce cytoplasmic and nuclear pools (3,42). Loss of E-cadherin in castrate

resistant prostate cancer leads to increased levels of β-catenin in the cytoplasm (43–45). Consistent with our results shown here, expressions of both AR and β-catenin have been reported to be elevated in castrate resistant prostate cancer (46,47). Increased expression of β-catenin could be mediated through the increased transcription (Figure 4A) and/or stabilization by Y142-phosphorylation (Figure 4B), decreased level of GSK3β and interaction with AR (Figure 5). Potential mechanisms of how β-catenin is able to enhance the transcriptional activity of the AR include facilitating the movement of the AR to the nucleus in response to androgen (15), modifying ligand requirement of the AR to utilize androstenedione and estradiol as agonists (2), and interactions with GRIP1, CARM1, p300 and FHL2 (reviewed in 48).

Activity of Wnt/β-catenin pathway in castrate resistant prostate cancer

The Wnt pathway and its interaction with AR have been suspected to play important roles in prostate cancer (48–50). In Fig 6 we illustrate changes in the expression levels of activators of β-catenin (Wnt2b, Yes1) that were increased (enlarged font size) while the inhibitors of β-catenin (Gsk3β, Ck1, Ck2, p53, Wnt5a and Plcβ) were decreased (reduced font size) in castrate resistant prostate cancer related to the androgen-dependent and/or androgen ablation samples as determined in these studies. These changes in expression would predict that β-catenin would dissociate from the cell membrane to facilitate its downstream transcription factors. However, expression of Tcf3 and Lef were also decreased. Competition for available β-catenin between Tcf3/Lef and AR has been suggested (21). Increased levels of β-catenin combined with decreased Tcf3/Lef would provide more β-catenin protein to be recruited by AR. Together these data suggest an increased pool of β-catenin would be available for potential interaction with other transcription factors such as AR. Other players in Wnt pathway may influence the transactivation of AR. These include GSK-3β (18–20) and cyclin D1 (22–24) that interact with the AR to repress AR activity. Decreased expression of GSK-3β and cyclin D1 as shown in this study could contribute the reactivation of AR pathway in castrate resistant prostate cancer.

Together these data provide a working model for a potential mechanism of progression to castrate resistant prostate cancer that involves aberrant expression of members of the Wnt pathway to promote the interaction between β-catenin and AR and thereby increase the transactivation of the AR to initiate transcription of genes normally regulated by androgen. Aberrant activation of the AR through the Wnt/β-catenin signaling pathway may play a role in the progression of prostate cancer to the castrate resistant state. Development of inhibitors that block protein-protein interactions between the AR and β-catenin may lead to viable therapies for this terminal stage of the disease.

Acknowledgements

We thank Nasrin R. Mawji for excellent technical support. This work was supported by funding from NIH, Grant R01 CA105304 (MDS) and a Michael Smith Foundation for Health Research Senior Graduate Studentship Award (GW).

References

1. Debes JD, Tindall DJ. Mechanisms of androgen-refractory prostate cancer. N Engl J Med 2004;351:1488–90. [PubMed: 15470210]
2. Truica CI, Byers S, Gelmann EP. Beta-catenin affects androgen receptor transcriptional activity and ligand specificity. Cancer Res 2000;60:4709–13. [PubMed: 10987273]
3. Yang F, Li X, Sharma M, et al. Linking beta-catenin to androgen-signaling pathway. J Biol Chem 2002;277:11336–44. [PubMed: 11792709]
4. Chesire DR, Ewing CM, Gage WR, Isaacs WB. In vitro evidence for complex modes of nuclear beta-catenin signaling during prostate growth and tumorigenesis. Oncogene 2002;21:2679–94. [PubMed: 11965541]

5. Voeller HJ, Truica CI, Gelmann EP. Beta-catenin mutations in human prostate cancer. Cancer Res 1998;58:2520–3. [PubMed: 9635571]
6. Polakis P. Wnt signaling and cancer. Genes Dev 2000;14:1837–51. [PubMed: 10921899]
7. Morin PJ. beta-catenin signaling and cancer. Bioessays 1999;21:1021–30. [PubMed: 10580987]
8. Ozawa M, Baribault H, Kemler R. The cytoplasmic domain of the cell adhesion molecule uvomorulin associates with three independent proteins structurally related in different species. Embo J 1989;8:1711–7. [PubMed: 2788574]
9. Eastman Q, Grosschedl R. Regulation of LEF-1/TCF transcription factors by Wnt and other signals. Curr Opin Cell Biol 1999;11:233–40. [PubMed: 10209158]
10. He TC, Sparks AB, Rago C, et al. Identification of c-MYC as a target of the APC pathway. Science 1998;281:1509–12. [PubMed: 9727977]
11. Tetsu O, McCormick F. Beta-catenin regulates expression of cyclin D1 in colon carcinoma cells. Nature 1999;398:422–6. [PubMed: 10201372]
12. Aberle H, Bauer A, Stappert J, Kispert A, Kemler R. beta-catenin is a target for the ubiquitin-proteasome pathway. Embo J 1997;16:3797–804. [PubMed: 9233789]
13. Molenaar M, van de Wetering M, Oosterwegel M, et al. XTcf-3 transcription factor mediates beta-catenin-induced axis formation in Xenopus embryos. Cell 1996;86:391–9. [PubMed: 8756721]
14. Verras M, Brown J, Li X, Nusse R, Sun Z. Wnt3a growth factor induces androgen receptor-mediated transcription and enhances cell growth in human prostate cancer cells. Cancer Res 2004;64:8860–6. [PubMed: 15604245]
15. Pawlowski JE, Ertel JR, Allen MP, et al. Liganded androgen receptor interaction with beta-catenin: nuclear co-localization and modulation of transcriptional activity in neuronal cells. J Biol Chem 2002;277:20702–10. [PubMed: 11916967]
16. Song LN, Herrell R, Byers S, Shah S, Wilson EM, Gelmann EP. Beta-catenin binds to the activation function 2 region of the androgen receptor and modulates the effects of the N-terminal domain and TIF2 on ligand-dependent transcription. Mol Cell Biol 2003;23:1674–87. [PubMed: 12588987]
17. Masiello D, Chen SY, Xu Y, et al. Recruitment of beta-catenin by wild-type or mutant androgen receptors correlates with ligand-stimulated growth of prostate cancer cells. Mol Endocrinol 2004;18:2388–401. [PubMed: 15256534]
18. Sharma M, Chuang WW, Sun Z. Phosphatidylinositol 3-kinase/Akt stimulates androgen pathway through GSK3beta inhibition and nuclear beta-catenin accumulation. J Biol Chem 2002;277:30935–41. [PubMed: 12063252]
19. Salas TR, Kim J, Vakar-Lopez F, et al. Glycogen synthase kinase-3 beta is involved in the phosphorylation and suppression of androgen receptor activity. J Biol Chem 2004;279:19191–200. [PubMed: 14985354]
20. Wang L, Lin HK, Hu YC, Xie S, Yang L, Chang C. Suppression of androgen receptor-mediated transactivation and cell growth by the glycogen synthase kinase 3 beta in prostate cells. J Biol Chem 2004;279:32444–52. [PubMed: 15178691]
21. Mulholland DJ, Read JT, Rennie PS, Cox ME, Nelson CC. Functional localization and competition between the androgen receptor and T-cell factor for nuclear beta-catenin: a means for inhibition of the Tcf signaling axis. Oncogene 2003;22:5602–13. [PubMed: 12944908]
22. Petre CE, Wetherill YB, Danielsen M, Knudsen KE. Cyclin D1: mechanism and consequence of androgen receptor co-repressor activity. J Biol Chem 2002;277:2207–15. [PubMed: 11714699]
23. Reutens AT, Fu M, Wang C, et al. Cyclin D1 binds the androgen receptor and regulates hormone-dependent signaling in a p300/CBP-associated factor (P/CAF)-dependent manner. Mol Endocrinol 2001;15:797–811. [PubMed: 11328859]
24. Petre-Draviam CE, Cook SL, Burd CJ, Marshall TW, Wetherill YB, Knudsen KE. Specificity of cyclin D1 for androgen receptor regulation. Cancer Res 2003;63:4903–13. [PubMed: 12941814]
25. Sadar MD, Akopian VA, Beraldi E. Characterization of a new in vivo hollow fiber model for the study of progression of prostate cancer to androgen independence. Mol Cancer Ther 2002;1:629–37. [PubMed: 12479223]
26. Wang G, Jones SJ, Marra MA, Sadar MD. Identification of genes targeted by the androgen and PKA signaling pathways in prostate cancer cells. Oncogene 2006;25:7311–23. [PubMed: 16751804]

27. Stamey TA, Yang N, Hay AR, McNeal JE, Freiha FS, Redwine E. Prostate-specific antigen as a serum marker for adenocarcinoma of the prostate. N Engl J Med 1987;317:909–16. [PubMed: 2442609]
28. Best CJ, Gillespie JW, Yi Y, et al. Molecular alterations in primary prostate cancer after androgen ablation therapy. Clin Cancer Res 2005;11:6823–34. [PubMed: 16203770]
29. Tusher VG, Tibshirani R, Chu G. Significance analysis of microarrays applied to the ionizing radiation response. Proc Natl Acad Sci U S A 2001;98:5116–21. [PubMed: 11309499]
30. Wang G, Sadar MD. Amino-terminus domain of the androgen receptor as a molecular target to prevent the hormonal progression of prostate cancer. J Cell Biochem 2006;98:36–53. [PubMed: 16440300]
31. Gregory CW, Hamil KG, Kim D, et al. Androgen receptor expression in androgen-independent prostate cancer is associated with increased expression of androgen-regulated genes. Cancer Res 1998;58:5718–24. [PubMed: 9865729]
32. Danilkovitch-Miagkova A, Miagkov A, Skeel A, Nakaigawa N, Zbar B, Leonard EJ. Oncogenic mutants of RON and MET receptor tyrosine kinases cause activation of the beta-catenin pathway. Mol Cell Biol 2001;21:5857–68. [PubMed: 11486025]
33. Piedra J, Miravet S, Castano J, et al. p120 Catenin-associated Fer and Fyn tyrosine kinases regulate beta-catenin Tyr-142 phosphorylation and beta-catenin-alpha-catenin Interaction. Mol Cell Biol 2003;23:2287–97. [PubMed: 12640114]
34. Gleave ME, Hsieh JT, von Eschenbach AC, Chung LW. Prostate and bone fibroblasts induce human prostate cancer growth in vivo: implications for bidirectional tumor-stromal cell interaction in prostate carcinoma growth and metastasis. J Urol 1992;147:1151–9. [PubMed: 1372662]
35. Cleutjens KB, van Eekelen CC, van der Korput HA, Brinkmann AO, Trapman J. Two androgen response regions cooperate in steroid hormone regulated activity of the prostate-specific antigen promoter. J Biol Chem 1996;271:6379–88. [PubMed: 8626436]
36. Riegman PH, Vlietstra RJ, van der Korput JA, Brinkmann AO, Trapman J. The promoter of the prostate-specific antigen gene contains a functional androgen responsive element. Mol Endocrinol 1991;5:1921–30. [PubMed: 1724287]
37. Schuur ER, Henderson GA, Kmetec LA, Miller JD, Lamparski HG, Henderson DR. Prostate-specific antigen expression is regulated by an upstream enhancer. J Biol Chem 1996;271:7043–51. [PubMed: 8636136]
38. Mousses S, Wagner U, Chen Y, et al. Failure of hormone therapy in prostate cancer involves systematic restoration of androgen responsive genes and activation of rapamycin sensitive signaling. Oncogene 2001;20:6718–23. [PubMed: 11709706]
39. Amler LC, Agus DB, LeDuc C, et al. Dysregulated expression of androgen-responsive and nonresponsive genes in the androgen-independent prostate cancer xenograft model CWR22-R1. Cancer Res 2000;60:6134–41. [PubMed: 11085537]
40. Zegarra-Moro OL, Schmidt LJ, Huang H, Tindall DJ. Disruption of androgen receptor function inhibits proliferation of androgen-refractory prostate cancer cells. Cancer Res 2002;62:1008–13. [PubMed: 11861374]
41. Li H, Kim JH, Koh SS, Stallcup MR. Synergistic effects of coactivators GRIP1 and beta-catenin on gene activation: cross-talk between androgen receptor and Wnt signaling pathways. J Biol Chem 2004;279:4212–20. [PubMed: 14638683]
42. Sasaki CY, Lin H, Passaniti A. Expression of E-cadherin reduces bcl-2 expression and increases sensitivity to etoposide-induced apoptosis. Int J Cancer 2000;86:660–6. [PubMed: 10797287]
43. Umbas R, Schalken JA, Aalders TW, et al. Expression of the cellular adhesion molecule E-cadherin is reduced or absent in high-grade prostate cancer. Cancer Res 1992;52:5104–9. [PubMed: 1516067]
44. Paul R, Ewing CM, Jarrard DF, Isaacs WB. The cadherin cell-cell adhesion pathway in prostate cancer progression. Br J Urol 1997;79(Suppl 1):37–43. [PubMed: 9088271]
45. de la Taille A, Rubin MA, Chen MW, et al. Beta-catenin-related anomalies in apoptosis-resistant and hormone-refractory prostate cancer cells. Clin Cancer Res 2003;9:1801–7. [PubMed: 12738737]
46. Chen CD, Welsbie DS, Tran C, et al. Molecular determinants of resistance to antiandrogen therapy. Nat Med 2004;10:33–9. [PubMed: 14702632]
47. Chen G, Shukeir N, Potti A, et al. Up-regulation of Wnt-1 and beta-catenin production in patients with advanced metastatic prostate carcinoma: potential pathogenetic and prognostic implications. Cancer 2004;101:1345–56. [PubMed: 15316903]

48. Verras M, Sun Z. Roles and regulation of Wnt signaling and beta-catenin in prostate cancer. Cancer Lett 2006;237:22–32. [PubMed: 16023783]

49. Mulholland DJ, Dedhar S, Coetzee GA, Nelson CC. Interaction of nuclear receptors with the Wnt/beta-catenin/Tcf signaling axis: Wnt you like to know? Endocr Rev 2005;26:898–915. [PubMed: 16126938]

50. Yardy GW, Brewster SF. Wnt signalling and prostate cancer. Prostate Cancer Prostatic Dis 2005;8:119–26. [PubMed: 15809669]

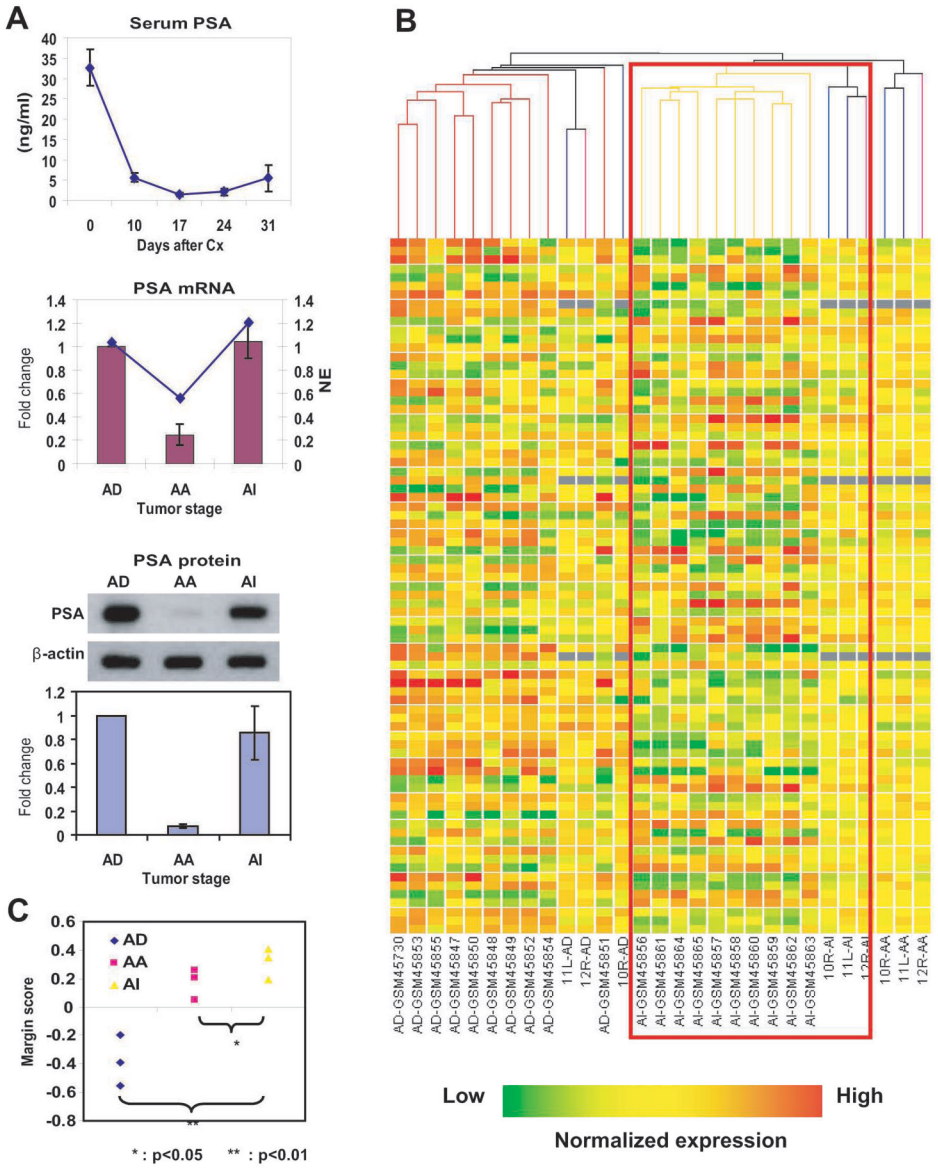

Fig. 1. The LNCaP hollow fiber model mimics hormonal progression of clinical prostate cancer

A, upper, Levels of serum PSA in at least three mice implanted with hollow fibers containing LNCaP cells after castration. Arrows indicate the times at which fibers were collected. *Middle*, Levels of PSA mRNA measured by Affymetrix (indicated by the line) and Q-PCR (columns) using total RNA harvested from hollow fibers from animals at the time points indicated by the arrows shown in *A*. Fold-change is based upon levels of PSA mRNA normalized to levels of GAPDH mRNA relative to levels of samples collected at day 0 (AD) and set at 1-fold. Samples are matched from the same animal at the different time points. AD signifies total RNA samples collected from animals immediately prior to castration at day 0 during growth in the presence of androgen. AA signifies RNA samples collected from animals 10 days after castration during androgen ablation and at the PSA nadir. AI represents RNA samples collected at day 31 after castration when PSA becomes re-expressed signifying castrate resistant growth. NE is the normalized expression. *Lower*, Western blot analysis of levels of PSA protein normalized to β-actin protein using whole cell lysates collected at the same time points as described above. Lower panel shows densitometry analysis of PSA protein

normalized to β-actin using matched samples from at least 3 different mice and set at 1-fold using the samples at day 0 (AD). *B,* Unsupervised clustering analysis of Affymetrix data using RNA samples collected from the hollow fiber model (n=9) with the clinical samples of prostate cancer (n=20) according to the 79 genes identified to be most significantly differentially expressed in castrate resistant versus androgen-dependent clinical samples, by standard correlation. The genes are represented by each row and the experimental samples are represented on each column. 10R/11L/12R are the identities of the 3 mice bearing fibers containing LNCaP cells. The suffix (AD, AA, or AI) represent when the sample was collected from the animal as described above. The red box highlights the cluster for AI samples (clinical and from the fiber model). *C,* Class prediction analysis to calculate the similarity of the fiber model samples to the clinical castrate resistant prostate cancer samples according to the expression pattern of the same group of genes depending of stage of hormonal progression (e.g, AD, AA, AI). Y-axis represents the margin scores to the castrate resistant clinical samples. Bars represent the mean ± standard deviation (SD).

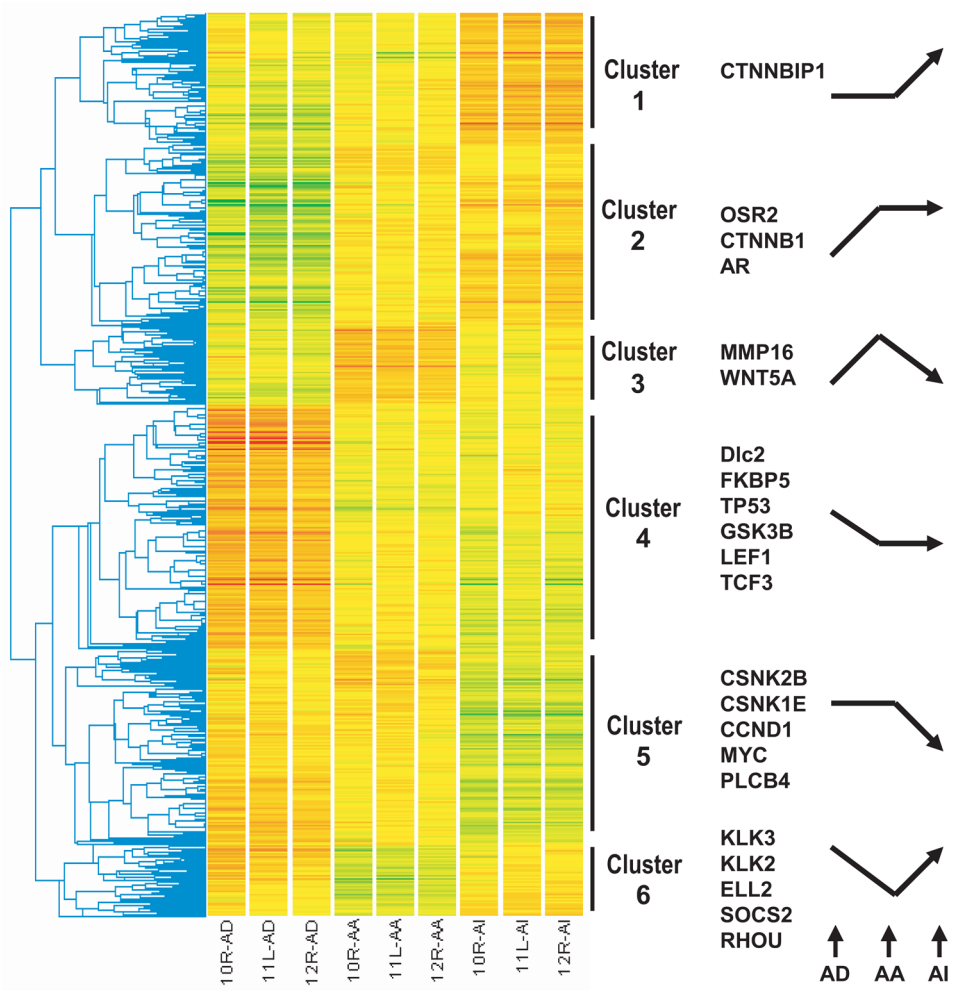

Fig. 2. Genes differentially expressed during the hormonal progression of prostate cancer in the hollow fiber model

Unsupervised clustering analyses of the 5667 genes according to their expression pattern during hormonal progression by standard correlation using the GeneSpring microarray analysis software. The genes are represented by each row and the experimental samples are represented on each column (in biological triplicates). Two-way ANOVA analysis of genes differentially expressed across all stages of progression ($p \leq 0.05$). The arrows represent the expression patterns of each cluster during hormonal progression from AD, to AA with castration, and finally AI. For example, expression of CTNNBIP1 does not change from AD to AA, but increases when AI.

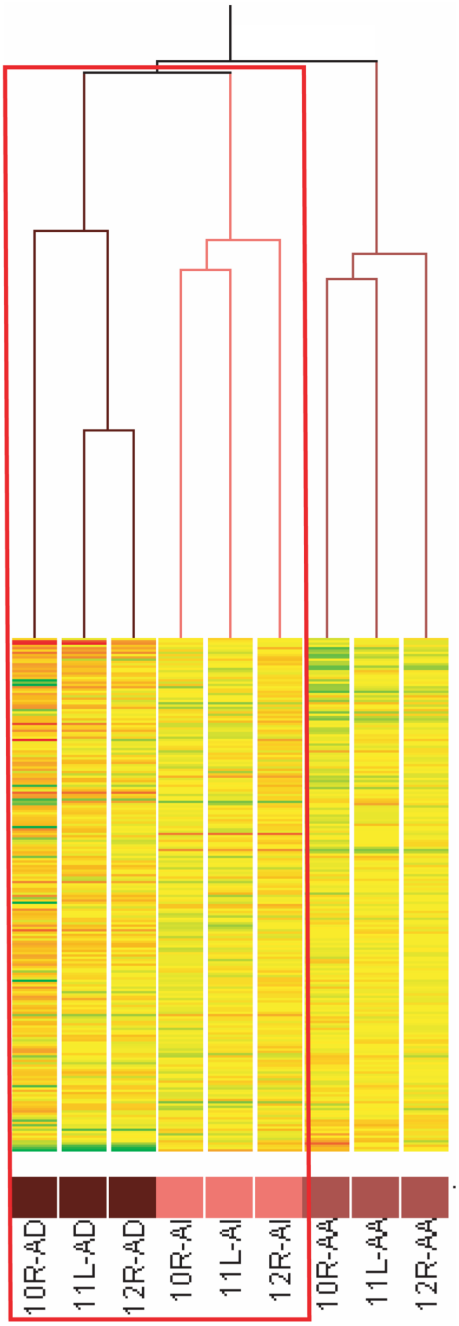

Fig. 3. Cluster analysis of the status of the androgen pathway in hormonal progression in the hollow fiber model

Unsupervised clustering analysis of samples harvested from the hollow fiber model (n=9) according to the 1092 genes identified to be androgen-regulated in a previous report (26), by standard correlation using the GeneSpring microarray analysis software. The genes are represented by each row and the experimental samples are represented on each column. 10R/11L/12R are the identities of the 3 mice bearing fibers containing LNCaP cells. The red box highlights the clustering of AD samples with AI samples.

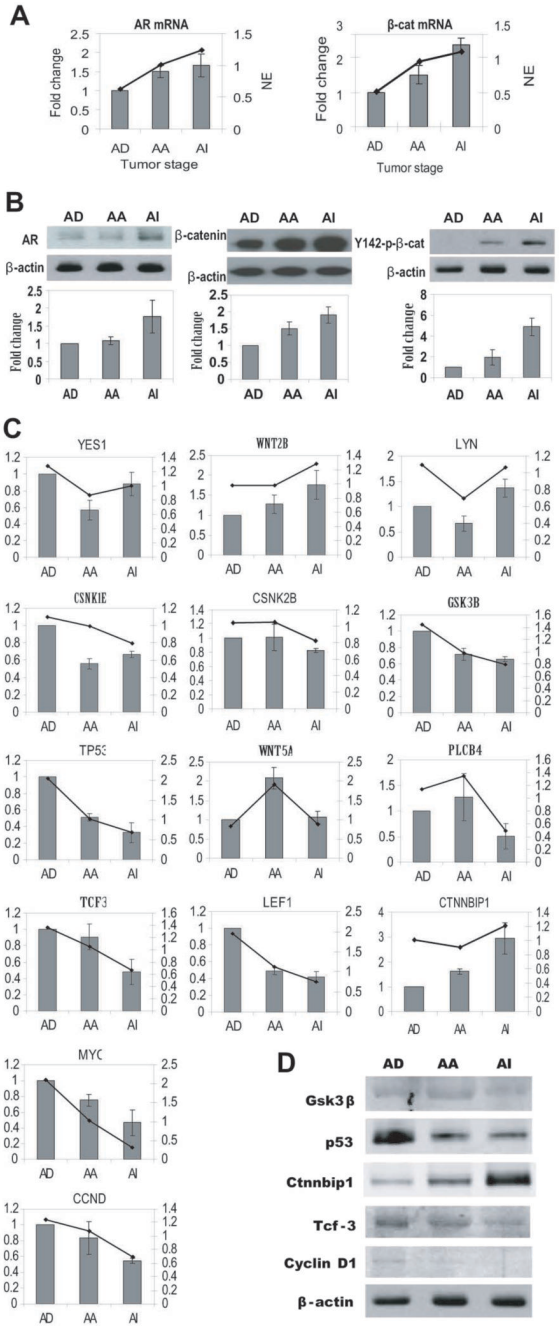

Fig. 4. Expression of AR, β-catenin, and regulators of b-catenin in the hollow fiber model

A, left, Levels of AR mRNA measured by Affymetrix (indicated by the line) and Q-PCR (columns) using total RNA harvested from the hollow fibers from animals at the time points indicated by the arrows shown in Fig 1*A*. Fold-change is based upon levels of AR mRNA normalized to levels of GAPDH mRNA relative to levels of samples collected at day 0 (AD) and set at 1-fold. *Right*, Levels of β-catenin mRNA in the fiber model measured by Affymetrix (line plot) and Q-PCR (column plot). *B, left*, Western blot analysis of levels of AR protein normalized to β-actin protein using whole cell lysates collected at the same time points as described above. Lower panel shows densitometry analysis of AR protein normalized to β-actin using matched samples from at least 3 different mice and set at 1-fold using the samples

at day 0 (AD). *Middle*, Western blot analysis of levels of β-catenin protein using the same samples as described in *C. Right*, Levels of Y142-phospho-β-catenin protein in these same samples. *C*, Levels of mRNAs of genes known to be involved in regulating β-catenin in samples harvested from the hollow fiber model measured by Affymetrix (line plot) and Q-PCR (column plot). AD, androgen dependent; AA, androgen ablation; AI, androgen-independent (castrate resistant); left Y-axis is the fold-change detected by Q-PCR; right Y-axis is the normalized expression (N.E.) for Affymetrix data; the bars represent the mean ± SD. *D*, Western blot analysis of protein levels of Gsk3β, p53, Tcf3, Ctnnbip1 and Cyclin D1using whole cell lysates collected at the same time points as described above. β-actin as the loading control.

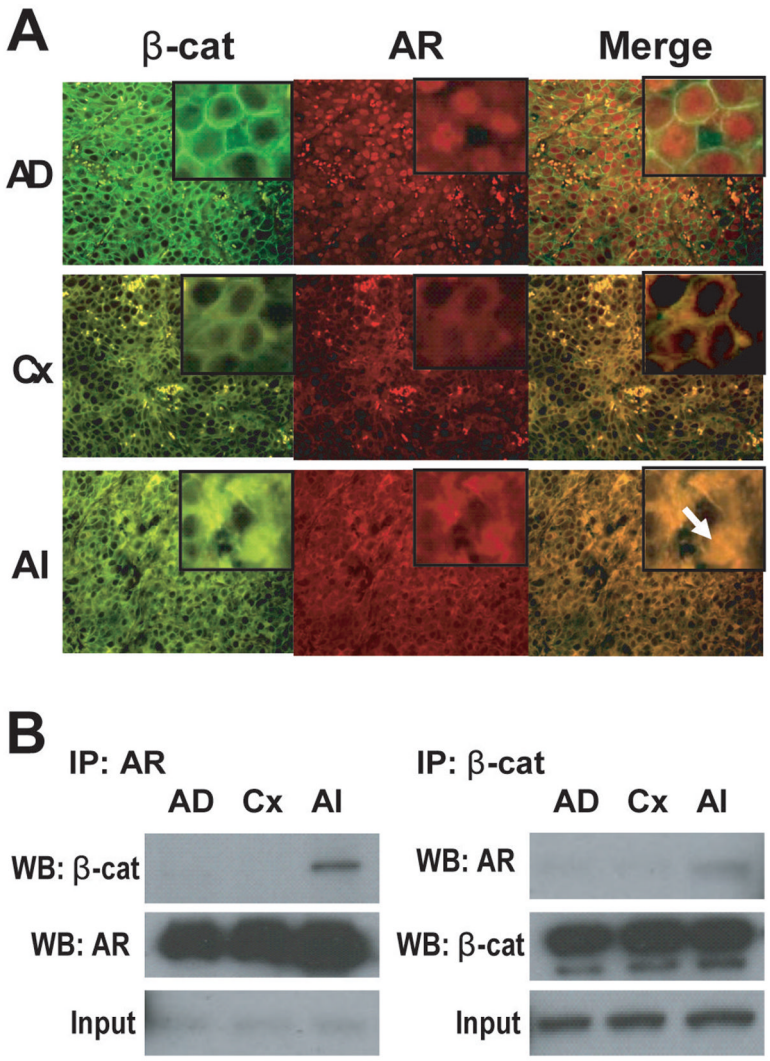

Fig. 5. Co-localization and endogenous interaction of AR and β-catenin in xenografts during hormonal progression in castrated mice

A, LNCaP xenografts were harvested from intact mice (AD); from mice 7 days after castration (Cx) at the PSA nadir; and when serum PSA indicated castrate resistance (AI) in castrated mice. Sections of xenografts were stained with antibodies against β-catenin (fluorescein isothiocyanate-labelled, green) together with antibodies against AR (tetramethylrhodamine isothiocyanate-labelled, red). Nuclear colocalization between AR and β-catenin (orange staining) is indicated by the white arrow. *B*, Co-immunoprecipitation of the endogenous complex of AR and β-catenin from xenografts harvested as described in *A*. Immunoprecipitations were performed using both anti-AR antibody (left) and anti-β-catenin antibody (right). Immune complexes were probed by western blot analyses as indicated in the figure.

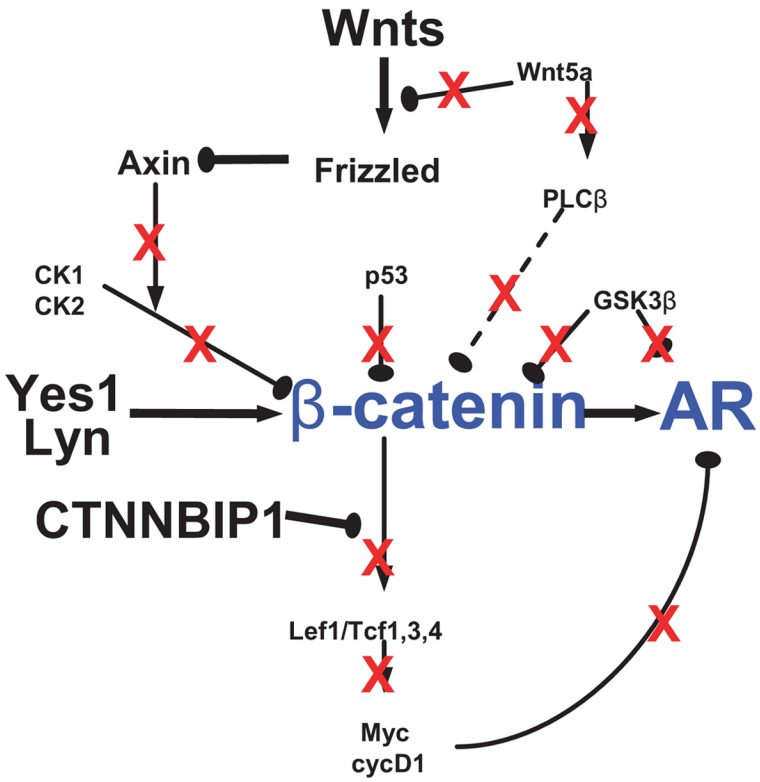

Fig. 6. Crosstalk between β-catenin and the AR in castrate resistant prostate cancer

The schematic shows differentially expression of members of the Wnt pathway in castrate resistant prostate cancer and the impact on AR transcriptional activity. See the text for a description.